# Numerical studies of turbulent wall-jets for mixing and combustion applications

by

Daniel Ahlman

November 2007
Technical Reports from
Royal Institute of Technology
Linné Flow Centre, Department of Mechanics
SE-100 44 Stockholm, Sweden

Akademisk avhandling som med tillstånd av Kungliga Tekniska Högskolan i Stockholm framlägges till offentlig granskning för avläggande av teknologie doktorsexamen fredagen den 14 december 2007 kl 10.15 i D3, Huvudbyggnaden, Kungliga Tekniska Högskolan, Lindstedtsvägen 5, entréplan, Stockholm.



Universitetsservice US–AB, Stockholm 2007

# Numerical studies of turbulent wall-jets for mixing and combustion applications

**Daniel Ahlman**
Linné Flow Centre, Dept. of Mechanics, Royal Institute of Technology
SE-100 44 Stockholm, Sweden

## Abstract

Direct numerical simulation is used to study turbulent plane wall-jets. The investigation is aimed at studying dynamics, mixing and reactions in wall bounded flows. The produced mixing statistics can be used to evaluate and develop models for mixing and combustion. An aim has also been to develop a simulation method that can be extended to simulate realistic combustion including significant heat release. The numerical code used in the simulations employs a high order compact finite difference scheme for spatial integration, and a low-storage Runge-Kutta method for the temporal integration. In the simulations the inlet based Reynolds and Mach numbers of the wall-jet are $Re = 2000$ and $M = 0.5$ respectively, and above the jet a constant coflow of 10% of the inlet jet velocity is applied. The development of an isothermal wall-jet including passive scalar mixing is studied and the characteristics of the wall-jet are compared to observations of other canonical shear flows. In the near-wall region the jet resembles a zero pressure gradient boundary layer, while in the outer layer it resembles a plane jet. The scalar fluxes in the streamwise and wall-normal direction are of comparable magnitude. In order to study effects of density differences, two non-isothermal wall-jets are simulated and compared to the isothermal jet results. In the non-isothermal cases the jet is either warm and propagating in a cold surrounding or vice versa. The turbulence structures and the range of scales are affected by the density variation. The warm jet contains the largest range of scales and the cold the smallest. The differences can be explained by the varying friction Reynolds number. Conventional wall scaling fails due to the varying density. An improved collapse in the inner layer can be achieved by applying a semi-local scaling. The turbulent Schmidt and Prandtl number vary significantly only in the near-wall layer and in a small region below the jet center. A wall-jet including a single reaction between a fuel and an oxidizer is also simulated. The reactants are injected separately at the inlet and the reaction time scale is of the same order as the convection time scale and independent of the temperature. The reaction occurs in thin reaction zones convoluted by high intensity velocity fluctuations.

**Descriptors:** wall-jet, direct numerical simulation, turbulence, non-isothermal, mixing, reaction, combustion

## Preface

In this thesis dynamics, mixing and reactions in plane turbulent wall-jets is studied by means of direct numerical simulation. The thesis is divided into two parts. In the first part the background and an overview of the research is presented. In the second part the research papers forming the base of the thesis are presented.

The thesis contains the following papers;

**Paper 1.** Ahlman D., Brethouwer G. and Johansson A. V., 2007 "Direct numerical simulation of a plane turbulent wall-jet including scalar mixing", *Physics of Fluids*, **19**

**Paper 2.** Ahlman D., Brethouwer G. and Johansson A. V., 2007 "Direct numerical simulation of non-isothermal turbulent wall-jets", Submitted to Physics of Fluids

**Paper 3.** Ahlman D., Brethouwer G. and Johansson A. V., 2007 "Direct numerical simulation of a reacting turbulent wall-jet", Technical Report, Linné Flow Centre, Dept. of Mechanics, KTH, Stockholm Sweden

**Paper 4.** Ahlman D., Brethouwer G. and Johansson A. V., 2007 "A numerical method for simulation of turbulence and mixing in a compressible wall-jet, version 2", Technical Report, Linné Flow Centre, Dept. of Mechanics, KTH, Stockholm Sweden

The papers are set in the present thesis format.

**Division of work between authors**
The research project was initiated by Arne Johansson (AJ) and Geert Brethouwer (GB) who have also acted as supervisors over the entire project. During the course of the work AJ, GB and Daniel Ahlman (DA) have continuously discussed the project progress and the results.

**Paper 1-3**
The code development needed to perform the simulations and to compute the statistics was performed by the DA. Subsequently the simulations and computation of statistics were also performed by DA. The evaluation of the results was done by DA with inputs from AJ and GB. The papers were written by DA and comments on the presentation and contributions to the discussions were provided by GB and AJ.

**Paper 4**
The simulation code was originally written by Bendiks Jan Boersma. The changes and development, described in the paper and in section 3.2 in Part I of the thesis, were performed by DA. The paper was written by DA with inputs from GB and AJ.

*Mänska! vill du livets vishet lära,*
*o, så hör mig! Tvenne lagar styra*
*detta liv. Förmågan att begära*
*är den första. Tvånget att försaka*
*är det andra. Adla du till frihet*
*detta tvång, och, helgad och försonad,*
*över stoftets kretsande planeter,*
*skall du ingå genom ärans portar.*

Utdrag ur *Suckarnas mystär* av
Erik Johan Stagnelius (1793–1823)

# Contents

# Part I

# Background and overview

CHAPTER 1

# Introduction

## 1.1. Turbulence and combustion

One of the most prominent features of turbulent flows is the diffusivity. The turbulent flow state rapidly mixes and transfers properties such as mass, momentum and heat. Turbulent mixing rates are significantly higher than mixing rates in laminar flows, where it occurs exclusively at the molecular level. In fact, turbulent diffusivity is the reason why we stir our cup of coffee after adding milk, to quickly mix it evenly. Relying on the slower molecular mixing would leave us waiting until the coffee have cooled off.

The diffusivity of turbulence also has important implications for combustion. In technical applications such as automobile engines or gas turbines, combustion nearly always takes place in turbulent flow fields. The main reason for this is that combustion is enhanced by the turbulence. Combustion, characterized by high rates of heat release, only occurs if the participating species are mixed to the right proportions on the molecular level. The high rates of transport and mixing inherently present in the turbulent environment, generate a faster combustion and energy conversion rate.

Already from this brief description it is evident that the reaction processes in turbulent combustion are strongly coupled to the flow field. Turbulence close to the flamefront may interact with the flame in a number of ways depending on the scale and strength of the turbulent fluctuation. Large, high intensity velocity fluctuations, convolute the flame, which increases the flame surface area and hence also the reaction rate. As the fluctuation scale becomes small and eventually of the order of the flame thickness it can enhance the mixing close to the flamefront but also quench it locally through high rates of strain.

Combustion processes also include heat release, which through buoyancy and gas expansion can generate instabilities and turbulence. Furthermore, when the temperature increases in the vicinity of the flame, owing to heat transfer from the reaction zone, the viscosity of the fluid increases and may locally modify the turbulence. The complex interaction of turbulence and reactions is exemplified in figure 1.1 where non-premixed ethylene flames in a round jet are seen for three different Reynolds numbers.

Gaseous turbulent combustion is subdivided into different régimes, based on the species initial mixing situation. The reaction processes are described as premixed, non-premixed or partially premixed turbulent combustion. In the


FIGURE 1.1. Soot emission photographs of round jet non-premixed ethylene flames with increasing inlet Reynolds numbers; $Re_o = 8200$ $(a)$, $Re_o = 15600$ $(b)$ and $Re_o = 24200$ $(c)$. From Muñiz & Mungal (2001).

premixed régime the participating species are assumed to be perfectly mixed before the ignition. This is generally the case in spark-ignition engines, where the fuel and oxidizer are mixed by turbulence for sufficiently long time, prior to the spark ignition of the mixture. Premixed flames also possess an inherent flame speed. As the reaction progresses in the premixed régime, the flame propagates relative to the unburnt mixture.

When fuel and oxidizer enter the combustion chamber in separate streams prior to reaction, the combustion is instead termed non-premixed. The flames present in this combustion régime are commonly referred to as diffusion flames, since diffusion processes are essential for bringing the fuel and oxidizer into contact. Contrary to flames in a premixed environment, diffusion flames do not possess an inherent flame speed. In aircraft turbines, the liquid fuel is injected into the combustion chamber. The liquid evaporates before it burns, typically in a non-premixed way in the form of diffusion flames. Incoming reactants from non-premixed streams must be continuously mixed and heated up by burnt gases, in order for the combustion to proceed. This process is referred to as flame stabilization and is often accomplished by creating recirculation zones. Intermediate to these canonical régimes is partially premixed combustion. This occurs when fuel and oxidizer are injected separately but are able to mix partially before ignition. This is generally the case in diesel engines.

Combustion of fossil fuels globally constitutes the dominating source of energy. Energy from other sources such as hydroelectric, solar, wind and nuclear energy account for less than 20% of the total energy production. Combustion of fossil fuel will therefore prevail as a key energy conversion technology at least in the next few decades. However, the negative environmental impacts of excessive fossil fuel combustion are becoming evident. Emissions of $CO_2$ contribute to global warming. Other pollutants such as unburnt hydrocarbons, soot and nitrogen oxides ($NO_x$) also have a negative impact on the environment. Nitrogen oxides in particular contribute to acidification, photochemical smog and influence the ozone balance in the stratosphere. More rigorous regulations concerning emissions are presently enforced in the automotive industry and on power plants to reduce emissions and environmental impact. To reach these goals, an improved understanding of combustion and mixing processes is needed, as well as improved models to be used in the development of cleaner combustion applications.

## 1.2. Mixing and combustion near walls

In power generation applications, combustion processes often take place in chambers. Inside these chambers some of the reaction and mixing is likely to occur close to and be affected by the solid enclosing walls. In the near-wall area, the interaction of the wall and the turbulent combustion is complex. These interactions are outlined in figure 1.2. Since the solid wall usually is significantly colder than the burning mixture, a heat flux is generated towards the wall which cools the mixture. This can lead to local flame quenching. In internal combustion engines, flame wall interaction is one of the dominant

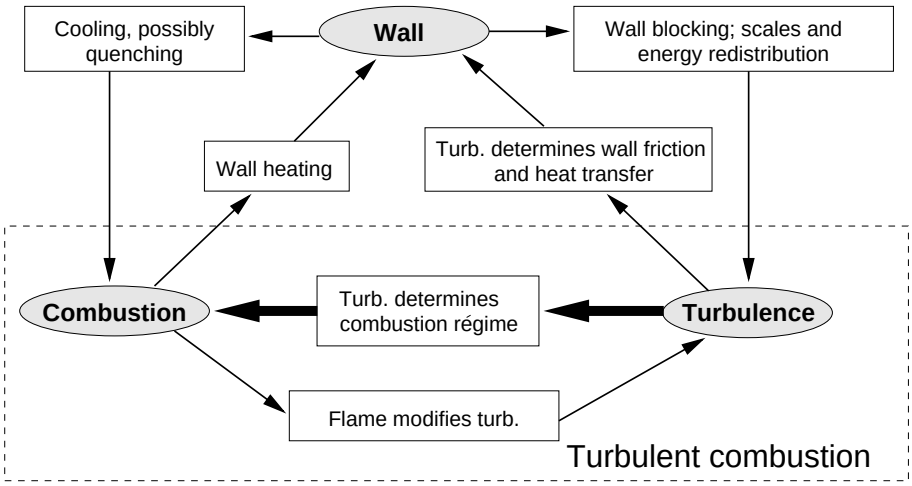


FIGURE 1.2. The interaction between the wall and the turbulent combustion (modified from Poinsot & Veynante (2001)).

sources of unburnt hydrocarbon emission. Another influence of the wall is on the mixing of the reacting components. Close to the wall turbulent fluctuations are damped, resulting in reduced mixing.

Clearly the wall influences the mixing and combustion in the vicinity of the wall in a profound way. It is therefore of interest to study processes in this region, and to add to the knowledge of the complex interaction. Simulations of mixing and combustion near walls are useful for a number of reasons. Accurate experiments in this region are difficult since the region of interest is very close to the wall. Highly resolved simulations can be used to support model development. Most combustion models are developed for isotropic conditions far from walls. It is not fully known how accurate the present models can capture wall effects on the mixing and combustion. Considering that walls have a profound impact, it is of interest to evaluate and develop accurate mixing and combustion models for the near-wall region.

The present thesis concerns the investigation of turbulent dynamics, mixing and reactions near a wall using direct numerical simulation. The study is part of a long term project, aimed at simulation of combustion near cold solid walls. In the present work, simulations of turbulent plane wall-jets have therefore been performed. Information on the mixing processes in wall-jets is of importance for evaluation and development of combustion models. In the second chapter further background to the research is presented. The role and application of direct numerical simulation to study turbulent combustion is considered. An overview of the area of combustion modelling is presented, where the importance of accurately representing the mixing situation is emphasized. In the final chapter the investigation in the present thesis is presented, including a background on turbulent wall-jets, the code development and a review of the simulations performed.

CHAPTER 2

# Numerical simulation of combustion

Numerical computation of turbulent flow phenomena is often divided into three categories in terms of the resolution of the computation. The highest level of resolution is used when solving the governing equations without resorting to models. This is referred to as direct numerical simulation (DNS). The application of DNS to combustion will be discussed below in section 2.1.

In large eddy simulation (LES) the large scales are resolved, while the smaller, unresolved scales, are accounted for by models. By reducing the resolved range of scales the computational effort is also reduced. As a result LES can be used to study higher Reynolds number flows which are unattainable using DNS. A review of the application of LES to combustion and its modelling issues is presented by Pitsch (2006).

The classical, and least computationally demanding approach, is to solve the fully averaged governing equations. The averaging however introduces higher order unclosed terms which have to be modelled. During the last decades, a wide variety of combustion models have been developed. Some of the more prominent models, presently used and still under development, include probability-density-function (pdf) models (Pope 1985), flamelet models (Peters 1986, 2000) and conditional moment closure methods (Klimenko & Bilger 1999). An overview of the state-of-the-art in combustion modeling has been published by Veynante & Vervisch (2002), but can also be found in Bilger (2000) and in the books of Poinsot & Veynante (2001) and Peters (2000). In section 2.2 a brief overview of turbulent combustion modelling, with an emphasis on mixing is presented.

## 2.1. Direct numerical simulation of combustion

### 2.1.1. *Governing equations*

In direct numerical simulation (DNS) of turbulent reacting flows the equations governing compressible flow and the transport equations of the participating species must be solved. Below the governing equations of a compressible reacting multicomponent fluid, containing $n$ species, are presented. The notation follows Poinsot & Veynante (2001) and the derivations of the equations, based on conservation of mass, momentum and energy, can be found in reference works such as Williams (1985) and Kou (2005).

2.1.1.1. *Conservation of mass and momentum*

Global conservation of mass and momentum are governed by

$$\frac{\partial \rho}{\partial t} + \frac{\partial \rho u_j}{\partial x_j} = 0 \tag{2.1}$$

$$\frac{\partial \rho u_i}{\partial t} + \frac{\partial \rho u_i u_j}{\partial x_j} = -\frac{\partial p}{\partial x_i} + \frac{\partial \tau_{ij}}{\partial x_j} + \rho \sum_{k=1}^{n} \theta_k f_{k,i} \tag{2.2}$$

where $\rho$ is the total mass density, $u_i$ is the velocity components, $p$ is the pressure, $\tau_{ij}$ is the viscous stress tensor, $\theta_k = m_k/m$ is the mass fraction of species $k$ and $f_{k,i}$ is the volume force acting on species $k$ in direction $x_i$. For a Newtonian fluid the viscous stress tensor is defined as

$$\tau_{ij} = \mu \left( \frac{\partial u_i}{\partial x_j} + \frac{\partial u_j}{\partial x_i} \right) - \mu \frac{2}{3} \frac{\partial u_k}{\partial x_k} \delta_{ij} \tag{2.3}$$

where $\mu$ is the dynamic viscosity. For a mixture of perfect gases the total pressure is governed by the ideal gas law

$$p = \rho \frac{\mathcal{R}}{W} T \tag{2.4}$$

where $\mathcal{R}$ is the universal gas constant and $W$ is the mean molecular weight of the mixture.

2.1.1.2. *Conservation of energy*

The total energy of the fluid per unit mass is defined as

$$e_t = e + \frac{1}{2} u_i u_i \tag{2.5}$$

where $e$ is the specific internal energy defined as

$$e = \sum_{k=1}^{n} h_k \theta_k - \frac{p}{\rho} \tag{2.6}$$

and $h_k$, the enthalpy of species $k$ at temperature $T$, is defined as

$$h_k = \Delta h^0_{f,k} + \int_{T^0}^{T} c_{p,k} dT. \tag{2.7}$$

Here $\Delta h^0_{f,k}$ is the mass enthalpy of formation of species $k$ at temperature $T^0$ and $c_{p,k}$ is the specific heat capacity at constant pressure. For a non-reacting single component fluid with constant heat capacities (calorically perfect) the internal energy and enthalpy can be specified as

$$e = c_v T, \quad h = c_p T. \tag{2.8}$$

The conservation of $e_t$ is governed by

$$\frac{\partial \rho e_t}{\partial t} + \frac{\partial \rho e_t u_i}{\partial x_i} = -\frac{\partial q_i}{\partial x_i} + \frac{\partial ((\tau_{ij} - p\delta_{ij}) u_i)}{\partial x_j} + \dot{\mathcal{Q}} + \rho \sum_{k=1}^{n} \theta_k f_{k,i} (u_i + V_{k,i}) \tag{2.9}$$

where $q_i$ is the heat flux in the $x_i$-direction, $\dot{\mathcal{Q}}$ is the heat added by external sources (e.g. an electric spark) and $V_{k,i}$ is the $x_i$-component of the diffusion velocity of species $k$. The last term on the right hand side describes the power produced by volume force $f_k$. The heat flux is

$$q_i = -\lambda \frac{\partial T}{\partial x_i} + \rho \sum_{k=1}^{n} h_k \theta_k V_{k,i} \tag{2.10}$$

which includes heat diffusion according to Fourier's law and a second term due to diffusion of species with different enthalpies. Concentration gradients may introduce an additional heat flux (the Dufour effect), but this contribution is in most cases negligible.

#### 2.1.1.3. *Conservation of species mass*

Each of the species $k$ involved in the reaction obeys a mass transport equation of the form

$$\frac{\partial \rho \theta_k}{\partial t} + \frac{\partial}{\partial x_i}\left(\rho \theta_k u_i\right) = -\frac{\partial \rho V_{k,i} \theta_k}{\partial x_i} + \dot{\omega}_k \tag{2.11}$$

where $V_{k,i}\theta_k$ is the diffusive flux in the $i$-direction, and $\dot{\omega}_k$ is the mass reaction rate describing the rate of creation or destruction of the species. Diffusive fluxes are caused by a number of transport processes on the molecular level. Accounting for all these is often too computationally expensive. The most common approximation is to assume that the fluxes follow Fick's law

$$V_{k,i}\theta_k = -\mathcal{D}_k \frac{\partial \theta_k}{\partial x_i} \tag{2.12}$$

where $\mathcal{D}_k$ is the binary diffusion coefficient of species $k$. From conservation of mass the sum of all $k$ fluxes should vanish $\sum_{k=1}^{n} V_{k,i}\theta_k = 0$, while the sum of the mass fractions is $\sum_{k=1}^{n} \theta_k = 1$. Global mass conservation is therefore violated when applying Fick's law and non-equal diffusivities in a multicomponent system.

### 2.1.2. *Mass reaction rate; general form*

The mass reaction rate $\dot{\omega}_k$ is dictated by the reaction mechanism under consideration. Here the description of $\dot{\omega}_k$ for a general mechanism is presented, and below a simplified reaction between a fuel and oxidizer species is considered.

Any one-step reaction of arbitrary complexity involving $n$ species can be described by

$$\sum_{k=1}^{n} \nu_k^r (M_k) = \sum_{k=1}^{n} \nu_k^p (M_k) \tag{2.13}$$

where $(M_k)$ denotes the concentration of species $k$ in moles per unit volume, $\nu_k^r$ are the stoichiometric coefficients of the reactants and $\nu_k^p$ the stoichiometric coefficients of the products. When a species does not occur as a reactant or product the corresponding coefficient is zero.

The rate of disappearance of species $k$ in an elementary reaction is governed by the law of mass action, stating that it is proportional to the product of the concentrations of the reacting species, where each species is raised to the power of the stoichiometric constant. The law of mass action can be verified experimentally (Glassman 1996) and was first proposed by Guldberg & Waage (1864). The reaction rate $R_k$ is hence given by

$$R_k = k \prod_{j=1}^{n} (M_j)^{\nu_j^r} \tag{2.14}$$

where $k$ is the called the specific rate coefficient. The sum $\sum \nu_k^r$ is referred to as the overall order of the reaction, and the single $\nu_k^r$ is the order of the reaction with respect to species $k$.

The rate of change of the concentration of species $k$ for a reaction with both forward and reversible propagation becomes

$$\dot{w}_k = \frac{d}{dt}(M_k) = \nu_k^{pr} k_{fv} \prod_{j=1}^{n} \left( \frac{\rho \theta_j}{W_j} \right)^{\nu_j^r} - \nu_k^{pr} k_{bk} \prod_{j=1}^{n} \left( \frac{\rho \theta_j}{W_j} \right)^{\nu_j^p} \tag{2.15}$$

where

$$\nu_k^{pr} = (\nu_k^p - \nu_k^r). \tag{2.16}$$

Here $W_k$ is the mean molecular weight and $k_{fv}$ and $k_{bk}$ denote the forward and backward rate coefficients respectively.

Reactions generally proceed though the formation of reactive intermediate species and possibly through different or parallel pathways. The overall reaction can however be represented as a series of elementary reactions, all of the form above, collectively called the reaction mechanism. If the number of reactions in the mechanism is $m$, then the source term in the species equation 2.11 is the sum over all reactions

$$\dot{\omega}_k = W_k \sum_{i=1}^{m} \dot{w}_{k,i} \tag{2.17}$$

which equals the total mass of the species produced per unit volume and time.

Arrhenius (1889) postulated that only molecules possessing energy exceeding a certain threshold, the activation energy $E_a$, would react when colliding. A temperature dependence of the specific reaction rate of the form

$$k = A(T) \exp\left( -\frac{E_a}{RT} \right). \tag{2.18}$$

is therefore called the Arrhenius law. The exponential term is the Boltzmann factor which from kinetic theory can be seen to give the fraction of all collisions that have an energy greater than $E_a$. The pre-exponential factor is the collision frequency, and in general $A(T) = AT^b$ is used to account for a mild temperature dependence.

### 2.1.3. *Mass reaction rate; simple reaction*

A simple irreversible reaction between an oxidizer $O$ and a fuel species $F$ forming a product $P$ can be described by

$$aO + bF \longrightarrow cP. \tag{2.19}$$

The rate of change of the species concentration, according to the section above, becomes

$$-\frac{1}{a}\dot{w}_o = -\frac{1}{b}\dot{w}_f = \frac{1}{c}\dot{w}_p = k\left(\frac{\rho\theta_o}{W_o}\right)^a\left(\frac{\rho\theta_f}{W_f}\right)^b \tag{2.20}$$

where $k$ is the reaction rate, which if temperature dependent can be specified by the Arrhenius Law defined above. If stoichiometric constants of one, $a = b = c = 1$, are used and the molecular weights of the reactants are $W$, then the reaction rates of the species becomes

$$-\dot{\omega}_o = -\dot{\omega}_f = \frac{1}{2}\dot{\omega}_p = \frac{k\rho^2}{W}\theta_o\theta_f. \tag{2.21}$$

### 2.1.4. *The role of DNS and experiments*

In the last three decades DNS has emerged as a very valuable tool in the study of turbulent mixing and combustion phenomena. Increasing computational resources have facilitated high resolution simulations, but also simulation of more complex phenomena including that of fluid dynamics coupled with reactions using detailed chemistry.

The benefit of DNS in investigations of mixing and combustion is that it provides access to the complete solution, because all length and time scales are resolved. Statistics of higher order, such as correlations, probability density functions and conditional averages can therefore be computed anywhere in the computational domain. The resolution of all scales is the main advantage of DNS but also results in its largest disadvantage, namely a high computational cost. DNS of engineering applications is therefore not possible. The range of length and time scales typically present in these means that DNS is too computationally demanding, even for the foreseeable future.

In simulations of reacting flows, the description of the reactions also has to be simplified. A complete mechanism for the simple reaction of hydrogen and oxygen gas typically involves 19 reactions and 9 species (Conaire *et al.* 2004). The combustion of a primary reference fuel (PRF) of iso-octane and n-heptane, used to evaluate the octane number of gasoline, is described by a mechanism of 4238 reactions and 1034 species (Curran *et al.* 2002). Considering the computational limitation, DNS should be regarded as a useful, and highly important, tool for model development and evaluation. Highly resolved simulations of simplified model problems can produce information on how to construct accurate models, and can be used to test which model approach provides the most accurate prediction. The progress in the application of DNS to study premixed turbulent and non-premixed combustion has been reviewed by Poinsot *et al.* (1996) and Vervisch & Poinsot (1998) respectively. Bilger (2000)

presented an overview of the issues of current interest in turbulent combustion, including the status and outlook of present computational models. The application of detailed chemistry and transport models was reviewed and discussed by Hilbert *et al.* (2004). Recently Westbrook *et al.* (2005) reviewed the progress in computational combustion over the last 50 years and illustrated the current capabilities of DNS.

Experimental techniques have also exhibited a fast evolution. The advent of laser measurement techniques has allowed for the development of very fast and accurate measurements. Using laser measurements reaction phenomena can be studied either in an idealized flow situation, or in some cases directly in the technical application. Example of the latter are Verbiezen *et al.* (2007) where the in-cylinder NO concentration is measured in a diesel engine and Seyfried *et al.* (2005) where Laser-Induced Fluorescence (LIF) and Laser-Induced Phosphorescence (LIP) was applied in the afterburner of a fighter-jet. In comparison to simulations, experimental investigations in general provide more localized information.

### 2.1.5. *DNS of turbulent reactive flows*

Riley *et al.* (1986) were probably the first to perform a three-dimensional DNS of a turbulent flow including chemical reactions. They studied a single irreversible non-premixed reaction in a turbulent mixing layer between an oxidizer and a fuel species disregarding heat release. Building on this work McMurtry *et al.* (1989) performed simulations including moderate heat release. Miller *et al.* (1994) also considered the reacting mixing layer, with low heat release, and carried out simulations for various Damköhler numbers (the ratio of the mixing time scale to the reaction time scale). Tanahashi *et al.* (2000) used detailed chemistry mechanism involving 12 species and 27 reactions in a DNS of premixed hydrogen/air combustion in homogeneous turbulence. Pantano *et al.* (2003) studied a reacting shear layer with heat release. They considered the infinitely fast reaction limit ($Da \to \infty$) by assuming that the reactions take place at a Burke-Schumann sheet at stoichiometric proportions. Pantano (2004) used DNS to study a turbulent non-premixed jet with finite rate chemistry. In this study a four step mechanism of methane and air combustion (Peters 1985) including eight chemical species was used and the dynamics of diffusion flame edges including extinction was studied. Premixed turbulent combustion in decaying homogeneous turbulence was studied by DNS by Treurniet *et al.* (2006). The flame front was modelled with a level set approach by a G-equation and the DNS was able to reproduce the hydrodynamical stability of the flame front. An example of a recent massive computation is that of Mizobuchi *et al.* (2005), where a hydrogen lifted flame was studied by DNS. In the simulation a round jet with a velocity of 680m/s was injected through a hole with a diameter of 2mm. The resulting Reynolds and Mach numbers were $Re = 13600$ and $M = 0.54$, and a reaction mechanism with 9 species and 17 reactions was used.

The lifted flame contained different flame elements; leading edge flames, inner rich premixed flames and outer diffusion flame islands.

#### 2.1.6. *DNS of reactive near-wall flows*

Studies of combustion near walls employing DNS include Poinsot *et al.* (1993) who studied flame-wall interaction of laminar and premixed combustion using compressible two-dimensional DNS and a simple reaction. Bruneaux *et al.* (1996) performed incompressible three-dimensional simulations of premixed combustion in a channel using a simple reaction. They found that quenching distances decrease and maximum heat fluxes increase in comparison to those of laminar flames. Their DNS data was also used in Bruneaux *et al.* (1997) to develop and evaluate a flame surface density model. Using a complex reaction mechanism consisting of 18 reactions involving 8 species, one-dimensional premixed and non-premixed flame interaction with an inert wall was simulated by Dabrieau *et al.* (2003). Wang & Trouvé (2005) used DNS to study flame structure and extinction events of non-premixed flames interacting with a cold wall. Their simulation was fully compressible, two-dimensional and the reaction was described using a single step model containing four species.

## 2.2. Combustion modelling

#### 2.2.1. *Averaged conservation equations*

Reacting flows in general include heat release and significant density fluctuations. This has implications for the averaging of the governing equations. When averaging the conservation equations for constant density flows, Reynolds decomposition of the flow variables, into a mean $\bar{f}$ and fluctuating $f'$ component, is conventionally used. Applying this to flows with varying density introduces unclosed correlations involving the fluctuating density of the type $\overline{\rho' f'}$. To reduce the number of unclosed terms, mass-weighted averages, also called Favre averages, are usually employed. Favre decomposition of an instantaneous variable $f$ is performed through

$$f = \frac{\overline{\rho f}}{\bar{\rho}} + f'' = \widetilde{f} + f'' \tag{2.22}$$

where $\widetilde{f}$ denotes the mass-weighted mean and $f''$ the corresponding fluctuating part. Using this decomposition and formalism, the averaged equations for conservation of mass, momentum and the mass fractions of species $k = 1, \ldots, N$ involved in the reaction become

$$\frac{\partial \bar{\rho}}{\partial t} + \frac{\partial}{\partial x_i}(\bar{\rho}\widetilde{u}_i) = 0 \tag{2.23}$$

$$\frac{\partial \bar{\rho}\widetilde{u}_i}{\partial t} + \frac{\partial}{\partial x_j}(\bar{\rho}\widetilde{u}_i\widetilde{u}_j) = -\frac{\partial \bar{p}}{\partial x_i} + \frac{\partial}{\partial x_j}\left(\bar{\tau}_{ij} - \overline{\rho u_i'' u_j''}\right) \tag{2.24}$$

$$\frac{\partial \bar{\rho}\widetilde{\theta}_k}{\partial t} + \frac{\partial}{\partial x_i}(\bar{\rho}\widetilde{u}_i\widetilde{\theta}_k) = \frac{\partial}{\partial x_i}\left(\overline{\rho \mathcal{D}_k \frac{\partial \theta_k}{\partial x_i}} - \overline{\rho u_i'' \theta_k''}\right) + \overline{\dot{\omega}}_k \tag{2.25}$$

The Favre averaged equations are formally identical to the Reynolds averaged equations for constant density flows. The unclosed terms appearing in the equations are the Reynolds stresses $\overline{\rho u_i'' u_j''}$, the scalar fluxes $\overline{\rho u_i'' \theta_k''}$ and the reaction source term $\overline{\dot{\omega}}_k$. Closure for the Reynolds stress term is usually achieved with a RANS-type turbulence model, e.g. a $k$–$\epsilon$ model.

An often used model for the scalar flux is formulated in terms of a classical gradient diffusion assumption

$$\overline{\rho u_i'' \theta_k''} = \bar{\rho}\widetilde{u_i'' \theta_k''} = -\frac{\mu_t}{Sc_{kt}} \frac{\partial \widetilde{\theta}_k}{\partial x_i} \tag{2.26}$$

where $\mu_t$ is the turbulent viscosity, estimated from the turbulence model, and $Sc_{kt}$ is the turbulent Schmidt number, which is usually of the order of one. In the case of reactive flows a gradient based model is a poor approximation for a number of reasons. The model fails at the reaction zone, where the reaction influences the scalar flux. Furthermore it is assumed that the scalar flux is aligned with the mean gradient, which in general is not true (Wikström *et al.* 2000).

Modeling the reaction source term $\overline{\dot{\omega}}_k$ can be regarded as the key difficulty in modeling turbulent combustion. The problem can be appreciated by studying the simple reaction $F + O \rightarrow P$. The mean reaction rate of the fuel species $F$ is of the form

$$\overline{\dot{w}}_F = -\overline{\rho^2 \theta_F \theta_O k} = -\overline{\rho^2 \theta_F \theta_O B e^{(-E_a/RT)}} \tag{2.27}$$

where $k(T)$ is the Arrhenius reaction rate constant and $E_a$ the activation energy of the reaction. The reaction rate is highly temperature dependent, which can have implications in computations in terms of stiffness of the solution. Also, the reaction rate is a function of the product of the instantaneous species concentrations, which can be termed as the mixing. In fact if the reaction rate is sufficiently fast, which it often is, the combustion rate depends directly on the mixing rate. The full expression is highly non-linear, indicating that modeling in terms of mean variables is not suitable.

### 2.2.2. *The eddy break up (EBU) model*

An early attempt to model the mean reaction rate was proposed by Spalding (1971). In premixed combustion the model is formulated in terms of the progress variable $c = (T - T_u)/(T_b - T_u)$ defined by the mixture temperature. The progress variable is 0 in the unburnt mixture ($T_u$) and 1 in the completely burnt mixture ($T_b$). Assuming that the reactions are sufficiently fast, the turbulent mixing becomes the rate-determining process, and the reaction rate is modelled as

$$\overline{\dot{\omega}} = \bar{\rho} C_{\text{EBU}} \frac{\sqrt{\widetilde{c''^2}}}{\tau_{\text{EBU}}} = \bar{\rho} C_{\text{EBU}} \frac{\epsilon}{k} \sqrt{\widetilde{c''^2}} \tag{2.28}$$

where $C_{\text{EBU}}$ is a model constant, $\tau_{\text{EBU}}$ is a characteristic time scale of the reaction and $c''^2$ is the variance of the progress variable. Since fast reactions are

assumed, the time scale is estimated to correspond to the integral time scale of the turbulent flow field $\tau_{\text{EBU}} = k/\epsilon$.

Also assuming that the flame is infinitely thin, the mixture temperature can only take two values since it is either fresh or fully burnt. In this case the mean reaction rate can be written as

$$\overline{\dot{\omega}} = \bar{\rho} C_{\text{EBU}} \frac{\epsilon}{k} \widetilde{c}(1 - \widetilde{c}) \tag{2.29}$$

in terms of the known mean quantities. Due to the simplicity of the description, the eddy break up model is used in most commercial combustion codes. The obvious limitation of the model is that no effects of chemical kinetics are included.

### 2.2.3. *Non-premixed combustion models*

To show how non-reacting scalars enter into models of combustion, examples from the modeling of non-premixed combustion are also presented here.

Models of non-premixed combustion are usually derived using a set of simplifying assumptions. Typical assumptions include constant and equal heat capacities for all species, low Mach numbers and unit Lewis numbers. Employing these assumptions, the flame position can be related to a single scalar quantity, $z$, termed the mixture fraction.

Using global conservation of species, linear combinations $Z_j$ of the species and temperature, that eliminates the source terms, can be constructed. If the coefficient of diffusivity $\mathcal{D}$ is assumed constant and equal for all species, then the scalars $Z_j$ are all governed by the same balance equation

$$\frac{\partial \rho Z_j}{\partial t} + \frac{\partial}{\partial x_i}\left(\rho u_i Z_j\right) = \frac{\partial}{\partial x_i}\left(\rho \mathcal{D} \frac{\partial \rho Z_j}{\partial x_i}\right) \tag{2.30}$$

Since the source term is eliminated, $Z_j$ are conserved scalars, subjected to diffusion and convection only. Reactions however plays an indirect role for the density and velocity fields by controlling the heat release. Normalization of the variables $Z_j$ can be performed through

$$z_j = \frac{Z_j - Z_j^O}{Z_j^F - Z_j^O} \tag{2.31}$$

where superscript $F$ denotes values in the fuel stream and $O$ values in the oxidizer stream. The normalized variables $z_j$ are governed by the same balance equation and subjected to the same boundary condition; $z_j = 1$ in the fuel stream and $z_j = 0$ in the oxidizer stream. Hence all normalized variables are equal, reducing the problem to the solution of one conserved scalar, the mixture fraction $z$.

In turbulent combustion models, the solution of the averaged mixture fraction is sought. Using Favre averaging this becomes

$$\frac{\partial \bar{\rho}\widetilde{z}}{\partial t} + \frac{\partial}{\partial x_i}(\bar{\rho}\widetilde{u}_i\widetilde{z}) = \frac{\partial}{\partial x_i}\left(\overline{\rho \mathcal{D} \frac{\partial z}{\partial x_i}} - \bar{\rho}\widetilde{u_i'' z''}\right). \tag{2.32}$$

In the averaged equation, the mixture fraction scalar flux $\widetilde{u_i''z''}$ is usually modelled using a gradient diffusion assumption of the form in (2.26). This gradient assumption is more justified for the mixture fraction, since it is a conserved scalar.

The mixture fraction is used in many models and the reason for this is that it provides a possibility to avoid the direct closure of the species source term, which was seen in section 2.2.1 to be a hard task. The definition of the mixture fraction can essentially be used to split the solution of the mean flame properties, the mixture fractions and the temperature, into two problems; a mixing problem and a flame structure problem. The first problem consists of describing the underlying mixing situation, which is provided from the mixture fraction. For an accurate description, both the mean field $\widetilde{z}$ and higher order statistics, preferably the full pdf $p(z)$, are needed. Usually at least the variance $\widetilde{z''^2}$ is provided. In the structure problem, the flame properties, mass fractions, temperature and species source terms, are recovered by using the mixture fraction information, i.e. the flame properties are expressed conditionally on the mixture fraction and its higher moments.

When $p(z)$ is known, the procedure to compute the average values, using the information of the underlying mixing can be expressed as

$$\bar{\rho}\widetilde{\theta}_k = \int_0^1 \left(\overline{\rho\theta_k|z^*}\right) p(z^*)dz^*, \quad \bar{\rho}\widetilde{T} = \int_0^1 \left(\overline{\rho T|z^*}\right) p(z^*)dz^* \tag{2.33}$$

$$\bar{\rho}\overline{\dot{\omega}}_k = \int_0^1 \left(\overline{\rho\dot{\omega}_k|z^*}\right) p(z^*)dz^*. \tag{2.34}$$

Here $z^*$ is used to represent the mixture fraction and its higher moments e.g. the scalar dissipation rate $\chi$ described in section 2.2.5. $(\overline{f|z^*})$ denotes the conditional average of the quantity $f$ for a set of mixture fraction statistics $z = z^*$.

In the flamelet model approach, the flame structure is characterized by the mixture fraction and the scalar dissipation rate at the reaction front $\chi_{st}$. Flame structure functions of the form $\theta_k(z, \chi_{st})$ are precalculated for laminar flames and stored in "flamelet libraries". The averaged property can then be computed from

$$\bar{\rho}\widetilde{\theta_k} = \int_0^\infty \int_0^1 \rho\theta_k(z, \chi_{st})p(z, \chi_{st})dzd\chi_{st} \tag{2.35}$$

where $p(z, \chi_{st})$ is the joint pdf of the mixture fraction and the scalar dissipation rate at the reaction front.

### 2.2.4. *Infinitely fast chemistry*

In the limit of infinitely fast chemistry, the combustion is determined solely by the mixing. Moreover, since the reaction is instant, the flame structure depends

only on the mixture fraction $z$. The mean quantities can be computed as

$$\bar{\rho}\widetilde{\theta}_k = \int_0^1 \rho\theta_k(z)p(z)dz, \quad \bar{\rho}\widetilde{T} = \int_0^1 \rho T(z)p(z)dz \tag{2.36}$$

The only unknown in the infinitely fast chemistry limit is thus $p(z)$. The determination of the pdf of the mixture fraction in a reacting mixture is still an open question. Two possible routes are to either estimate the pdf using an assumed shape, or to solve a transport equation for the pdf (Pope 1985). For engineering purposes the first possibility is often sufficient. The most common assumed pdf is the $\beta$-function, which is defined as

$$p(z) = \frac{z^{a-1}(1-z)^{b-1}}{B(a,b)} \tag{2.37}$$

where $B$ is a normalization function. The parameters $a$ and $b$ are determined from the mean $\widetilde{z}$ and variance $\widetilde{z''^2}$ of the mixture fraction as

$$a = \widetilde{z}\left(\frac{\widetilde{z}(1-\widetilde{z})}{\widetilde{z''^2}} - 1\right), \quad b = \frac{a}{\widetilde{z}} - a. \tag{2.38}$$

The structure of the pdf and also the complete flame is defined through the assumed pdf. The determination of the pdf requires information of the mixture fraction $\widetilde{z}$ and its variance $\widetilde{z''^2}$.

### 2.2.5. *Scalar variance transport equation*

The mean field value $\widetilde{z}$ describes the global location and the structure of the flame. For information of the local mixing situation, higher order statistics are needed. The mixture fraction variance $\widetilde{z''^2}$ provides the first level of information of the local mixing and most combustion models therefore require information on a scalar variance for closure. As was seen in the previous section, even in the limit of infinitely fast reactions using an assumed pdf approach, information on the passive scalar variance $\widetilde{z''^2}$ is needed. The scalar variance can be employed directly for closure in moment methods and in models employing assumed pdfs. Both models using the flamelet approach, and conditional moment closure models include assumed pdfs.

In the RANS approach the variance $\widetilde{z''^2}$ is obtained from a transport equation which reads

$$\begin{aligned}\frac{\partial\bar{\rho}\widetilde{z''^2}}{\partial t} + \frac{\partial}{\partial x_i}\left(\bar{\rho}\widetilde{u}_i\widetilde{z''^2}\right) = \\ \underbrace{-\frac{\partial}{\partial x_i}\left(\overline{\rho u_i'' z''^2}\right)}_{I} + \underbrace{\frac{\partial}{\partial x_i}\left(\overline{\rho\mathcal{D}\frac{\partial z''^2}{\partial x_i}}\right)}_{II} - \underbrace{2\overline{\rho u_i'' z''}\frac{\partial\widetilde{z}}{\partial x_i}}_{III} - \underbrace{2\overline{\rho\mathcal{D}\frac{\partial z''}{\partial x_i}\frac{\partial z''}{\partial x_i}}}_{IV}\end{aligned} \tag{2.39}$$

when $\mathcal{D}$ is constant. The various right hand side terms are identified as $(I)$ turbulent transport, $(II)$ molecular diffusion, $(III)$ production and $(IV)$ dissipation. Closing the equation requires models for all the right-hand-side terms.

For the turbulent transport, a gradient transport model of the form in (2.26) can be used. Molecular diffusivity is usually neglected, assuming sufficiently large Reynolds numbers. The scalar flux term in the turbulent production is also modeled using a gradient model.

The dissipation term identified ($IV$), often referred to as the scalar dissipation rate, is an important quantity in combustion modeling. The scalar dissipation rate is a direct measure of the fluctuation decay. This can be seen by considering homogeneous combustion, i.e. negligible mean mixture fraction gradients, in which case the mixture fraction balance equation reduces to

$$\frac{\partial \bar{\rho}\widetilde{z''^2}}{\partial t} = -2\overline{\rho\mathcal{D}\frac{\partial z''}{\partial x_i}\frac{\partial z''}{\partial x_i}} = -\bar{\rho}\widetilde{\chi}_f \tag{2.40}$$

which shows that the decay is fully governed by the turbulent micro-mixing in terms of the scalar dissipation rate. This is reflected in the nature of the non-premixed flames where fresh fuel and oxidizer have to be mixed on the molecular level and the reaction is mainly controlled by micro-mixing. A commonly used approach to model the scalar dissipation rate $\widetilde{\chi}_f$ is to relate it to the turbulence time scale $\tau_t$ as

$$\widetilde{\chi}_f = c\frac{\widetilde{z''^2}}{\tau_t} = c\frac{\epsilon}{k}\widetilde{z''^2} \tag{2.41}$$

where $k$ and $\epsilon$ are the turbulent kinetic energy and dissipation rate, and $c$ is a model constant in the order of one. The assumption implies that the respective scalar and turbulence time scales are proportional to each other.

The concept of scalar dissipation varies throughout the combustion literature. The main difference is whether it concerns the mean scalar or the fluctuation, i.e. $z$ or $z''$, in the turbulent non-premixed case. A total Favre averaged scalar dissipation rate $\widetilde{\chi}$ can be formulated as

$$\bar{\rho}\widetilde{\chi} = 2\overline{\rho\mathcal{D}\frac{\partial z}{\partial x_i}\frac{\partial z}{\partial x_i}} = 2\overline{\rho\mathcal{D}}\frac{\partial \widetilde{z}}{\partial x_i}\frac{\partial \widetilde{z}}{\partial x_i} + 4\overline{\rho\mathcal{D}\frac{\partial z''}{\partial x_i}\frac{\partial \widetilde{z}}{\partial x_i}} + 2\overline{\rho\mathcal{D}\frac{\partial z''}{\partial x_i}\frac{\partial z''}{\partial x_i}} \tag{2.42}$$

### 2.2.6. *Conclusion; scalar mixing*

In conclusion, scalar mixing can be stated to be of utmost importance in combustion modeling. In models of non-premixed combustion, the mixing is characterized by a single conserved scalar, the mixture fraction $\widetilde{z}$, and its higher order statistics. Scalar variances are often used in closures and in prescribed pdfs.

The scalar dissipation rate $\widetilde{\chi}$ is a key concept in combustion models, since it can be interpreted as a measure of the scalar fluctuation decay rate through turbulent micro-mixing. In fact, either $\widetilde{\chi}$ or a closely related quantity can be found in any model. Apart from the micro-mixing description, accurate modeling of the scalar flux term $\widetilde{u''z''}$ is also important, since it has a large influence on $\widetilde{z}$ and $\widetilde{z''^2}$. DNS can be used to develop combustion models and to evaluate presently used models since it can provide highly resolved information

on the scalar mixing. Of particular interest is to evaluate the scalar dissipation and the validity of gradient based closures of scalar fluxes.

CHAPTER 3

# Simulation of turbulent wall-jets

## 3.1. Wall-jet setup and background

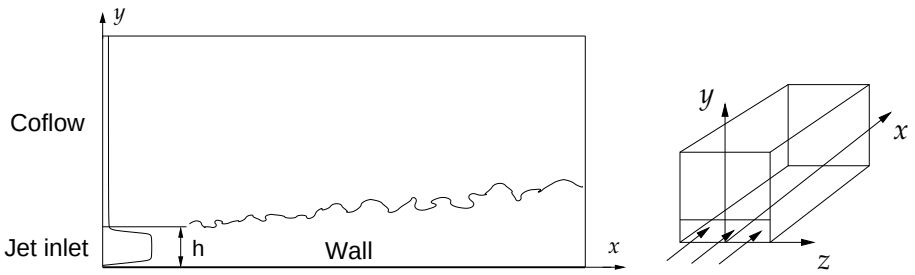


FIGURE 3.1. The plane wall-jet computational domain.

The flow configuration studied in this thesis is a plane turbulent wall-jet which is generated by injecting fluid with a velocity higher than the ambient flow along a flat solid wall. The flow configuration and the computational domain used in the simulations are depicted in figure 3.1. Two visualizations of wall-jet flow, one numerical and one experimental, are shown in figure 3.2. This setup was chosen since it is of interest both in engineering applications and from a theoretical view point. Plane wall-jets are used in mixing or cooling applications such as in turbine blade cooling, in windshield demisters and in flow control on airplane wings. Wall-jets also occur in combustion situations e.g. following fuel or hot exhaust gas impingement on solid walls. The dynamics of the wall-jet is interesting since it contains two different shear layers. The inner region from the wall to the jet center resembles a boundary layer, while the outer region resembles a free shear layer. The presence of the wall also profoundly influences mixing and combustion processes as was discussed in section chapter 1.

To this date a vast number of studies have been devoted to turbulent wall-jets. The majority of these are experimental investigations of which the very first was conducted by Förthmann (1936). Many of the key features of wall-jets were identified already in this study; the mean velocity develops in a self-similar manner, the half-width growth is linear and the maximum velocity decay is

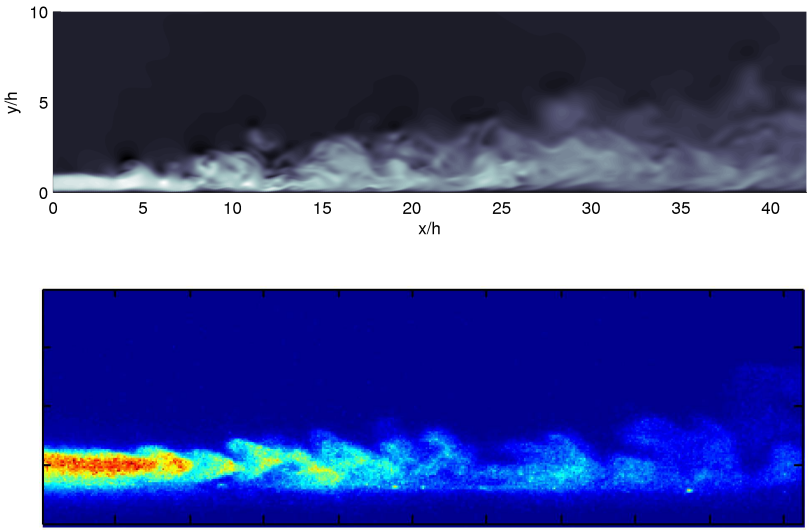


FIGURE 3.2. Visualizations of plane wall-jet flow. Above a snapshot of the simulated streamwise velocity (Ahlman *et al.* 2007*a*) and below a snapshot of an experimental wall-jet using LIF with acetone seeding (Ehn *et al.* 2007).

inversely proportional to the square root of the downstream distance. Bradshaw & Gee (1960) were the first to measure turbulence statistics in a wall-jet and concluded that the Reynolds shear stress is finite at the position of maximum velocity and zero closer to the wall. The experimental investigations of wall-jets carried out prior to 1980 have been compiled and critically reviewed by Launder & Rodi (1981, 1983). The most accurately resolved wall-jet experiment to date was reported by Eriksson *et al.* (1998). They studied a wall-jet with $Re = 9600$ in a large water tank (7m long and 1.45m wide) and used Laser Doppler Velocimetry (LDV) to measure the velocity into the viscous sublayer, which enabled direct determination of the wall shear stress.

Numerical studies of wall-jets are more scarce, but following the rapid increase in simulation power a number of studies have been reported over the last decade. The breakdown of a finite aspect ratio wall-jet was studied by Visbal *et al.* (1998). Levin *et al.* (2005) studied the wall-jet laminar breakdown using linear theory and DNS and presented averaged statistics from the turbulent region in a following paper (Levin *et al.* 2006). Dejoan & Leschziner (2005) performed a highly resolved large eddy simulation (LES) of a plan wall-jet, matching the experiment of Eriksson *et al.* (1998). The simulated mean velocities and the Reynolds stress agreed well with the experiment and an extensive study of the budgets of the kinetic energy and the Reynolds stress was carried out.

The first DNS of wall-jet flow including scalar mixing as well as the first DNS of non-isothermal wall-jets was carried out by Ahlman *et al.* (2007*a*,*b*).

Several studies have been devoted to scaling laws for the wall-jet statistics. A first choice is to use the inlet velocity and jet height as characteristic scales. This has however been found to introduce Reynolds number dependencies (see e.g. Launder & Rodi 1981). Narashima *et al.* (1973) suggested that the mean properties should scale with the inlet momentum flux and the kinematic viscosity. George *et al.* (2000) performed a similarity analysis of the inner and outer layers of the wall-jet. They found that neither inner nor outer scales give a complete collapse for finite Reynolds numbers. In conclusion, no single set of scales has been found that properly collapses the entire turbulent profiles. This can be understood as a result of the wide separation of scales inevitably present between the near-wall region and the outer shear layer. It can be argued that the turbulence in the inner region is governed by the wall boundary layer whereas the turbulence in the outer region is governed by the free shear layer. In correspondence characteristic scales near the wall tend to the viscous boundary layer scales, while in the outer shear layer the characteristic scales tend to the outer scales of a plane jet.

The aim of the present work has been to study dynamics, mixing and reactions in a plane wall-jet using direct numerical simulation. This work has included the development of a simulation method for the present configuration, and this development is outlined in the next section. Then a brief overview of self-similarity of turbulent flows in connection to wall-jets is presented. In the last section the three studies that have been carried out are discussed and some of the results are summarized.

## 3.2. Code development

In order to study plane turbulent wall-jets, a code for the direct numerical simulation of the Navier-Stokes equations and the transport equations of scalar species has been developed. The development has been incremental and all results presented in this thesis where produced using the code at different stages. Below the background of the code is given and the development is outlined.

The simulation code was originally written by Prof. Bendiks Jan Boersma[1], and has previously been used to study the sound field produced by a round jet in Boersma (2004). The overall solution procedure, the integration techniques and the method for parallel computation have been maintained from the original implementation. The numerical method includes compact finite difference schemes for the spatial integration and a Runge-Kutta method for the temporal integration. The simulation code solves the fully compressible equations governing fluid flow. To reduce reflections, boundary zones are applied at the in- and outlets. The numerical techniques and the implementation are described in detail in the enclosed Paper 4 (Ahlman *et al.* 2007*b*).

[1]Currently at Laboratory for Aero & Hydrodynamics, Delft University of Technology

The initial development of the code included changes of the computational domain and a redesign of the inlet and boundary conditions. At the top of the domain an entrainment inflow was devised, using information from the experimental results of Eriksson *et al.* (1998). A parallel coflow was added above the jet to advect large persistent vortices out of the computational domain, which would otherwise have affected the statistics. To perform mixing studies the transport equation of a passive scalar was implemented. The scalar is added in the jet and the scalar concentration is zero in the coflow. At the wall a no-flux condition is prescribed.

A method was developed to generate efficient inlet disturbances that promote fast transition to turbulence and thereby provide turbulent propagation in the main part of the computational domain. The disturbance includes three types of disturbances superimposed at the inlet; correlated disturbances, streamwise vortices and periodic streamwise forcing. Correlated disturbances are produced using a digital filter (Klein *et al.* 2003) using an assumed autocorrelation and a specified correlation length. The streamwise vortices are added in the upper shear layer of the wall-jet.

In the wall-jet simulations, the streamwise grid stretching is adjusted to decrease the node separation over the transition region, where strong disturbances are produced. A second order filter was developed and applied to the scalars (passive and reactive) over the transition region $x/h < 12$ to avoid negative concentrations in the outer part of the jet.

For the non-isothermal jet simulations, inlet profiles for the density and energy (temperature) were implemented. Realistic target functions for the density and energy at the outlet were also developed to minimize the downstream influence of the boundary zones.

For the reacting simulation two additional scalar transport equations, describing the oxidizer and fuel mass fractions, were implemented, including reaction terms and inlet profiles.

## 3.3. Self-similarity of turbulent flows

In the analysis of the turbulent wall-jet simulations the possibility of self-similarity of the statistics is investigated. A brief discussion of this concept is therefore in order.

Self-similarity or self-preservation (Tennekes & Lumley 1972) of turbulent flows is an important concept, both from a theoretical and an engineering view point, since it presents a simplified description of the flow development and statistics. Self-similar statistics have an increased generality, and can to higher degree be used for comparisons with related flow cases.

In simple flow geometries the flow development can sometimes be described using one or several local velocity and local time scales. This requires that the flow development is slow and that the turbulent time scales are small enough to adjust to the gradually developing flow structure. In the case of statistically two-dimensional flows, the flow can sometimes be found to be governed by a

single locally defined velocity and time scale. Examples of such flows are plane and round jets and wakes. In wall bounded shear flows the situation is more complex. At the wall the no-slip condition must be fulfilled i.e. the velocity of the fluid at the surface must be equal to that of the surface. To identify similarities in these flows the inner region, influenced by viscosity, and the rest of the flow, termed the outer layer, must be treated separately.

The turbulent wall-jet flow can be seen as a combination of two generic shear layers. The inner layer, extending from the wall out to the jet center, resembles a boundary layer, while the outer layer is similar to a plane jet. Both the boundary layer and the plane jet exhibit self-similar properties and below some consequences of these are presented.

### 3.3.1. *Law of the wall*

In wall bounded flows at high Reynolds numbers, an inner layer $\delta_w$, much thinner than the entire boundary layer $\delta$, is assumed to exist i.e. $\delta_w \ll \delta$. In this layer the mean velocity is governed by the viscosity, and is independent of $\delta$ and the free stream velocity $U_\infty$. It can then be argued that the mean velocity profiles should have the functional dependence

$$U = f(y, \tau_w, \rho, \nu) \tag{3.1}$$

where $y$ is the distance from the wall, $\tau_w = \rho\nu(\partial U/\partial y)_{y=0}$ is the wall shear stress and $\rho$ and $\nu$ are the density and kinematic viscosity of the fluid. Because only $\tau_w$ and $\rho$ depend on mass they can be combined to form a velocity scale $u_\tau = \sqrt{\tau_w/\rho}$. A characteristic viscous length scale can be formed in the manner of $l^* = \nu/u_\tau$. Dimensional analysis thus gives

$$U^+ = f(y^+) \tag{3.2}$$

where plus index properties are referred to as wall units and are defined as

$$U^+ \equiv U/u_\tau, \quad y^+ \equiv y/l^*. \tag{3.3}$$

Relation 3.2 is commonly termed *the law of the wall*. A vast number of experimental investigations in high Reynolds number flows have shown that the function $f(y^+)$ has universal form in both channel flow, pipe flow and in boundary layers.

At the wall the no-slip condition corresponds to $f(0) = 0$. A Taylor series expansion for small $y^+$ shows that the linear relation $U^+ = y^+$ is a good approximation in the near wall region. For zero pressure-gradient flows the next non-zero term can be shown to be $\mathcal{O}(y^{+4})$. Simulations and experimental studies of wall bounded flows in general show a good agreement with the linear relation for $y^+ < 5$ and this region is hence referred to as the *viscous sublayer*.

### 3.3.2. *Plane jets*

A plane turbulent jet is achieved experimentally by injecting high velocity fluid into a stationary region, through a rectangular slot of large aspect ratio, $h/L_z > 50$ say, where $h$ is the slot height and $L_z$ the spanwise slot width.

If the plane jet is assumed self-similar in terms of the local maximum velocity $U_m = U_m(x)$ and a local length scale $y_c = y_c(x)$, the mean streamwise velocity and the Reynolds stress can be defined by

$$\bar{U}(x,y) = U_m(x) f(\eta) \tag{3.4}$$

$$\overline{uv}(x,y) = U_m^2(x) g(\eta) \tag{3.5}$$

$$\eta \equiv y/y_c(x) \tag{3.6}$$

where $x$ and $y$ denotes the mean flow direction cross stream direction respectively. Inserting these relations into the boundary layer equation and neglecting the viscous term, the following relation is obtained (Pope 2000)

$$\frac{1}{2}\frac{dy_c}{dx}\left(f^2 + f'\int_0^\eta f d\eta\right) = g'. \tag{3.7}$$

Both the left hand side parenthesis and the right hand side term are independent of $x$, implying that $dy_c/dx$ must also be independent of $x$, i.e. the growth rate of $y_c$ is constant. Integrating the boundary equation in the wall-normal direction, the momentum flux, per unit span, is

$$\frac{d\dot{M}}{dx} = \frac{d}{dx}\left(\rho U_m(x)^2 y_{1/2}(x)\int_{-\infty}^{\infty} f(\eta) d\eta\right) = 0 \tag{3.8}$$

and hence conserved. A constant growth rate therefore implies that the maximum velocity must vary as $U_m \sim x^{-1/2}$.

The mean streamwise profile and the Reynolds stress profiles obtained in experiments (see e.g. Gutmark & Wygnanski 1976) collapse (i.e. profiles at increasing downstream position fall on top of each other) when scaled by the maximum velocity $U_m$ and the half-width position $y_{1/2}$ defined as

$$\bar{U}(x, y_{1/2}(x), 0) = \frac{1}{2}U_m \tag{3.9}$$

The collapse occurs beyond a position of about $x/h = 40$, indicating that some distance from the inlet is needed for the flow to become independent of the initial conditions. Downstream of the initial region, the growth rate of the half-width is constant i.e. $dy_{1/2}/dx \sim S$, usually $S \approx 0.1$ is reported. The development of the maximum velocity follows $U_m \sim x^{-1/2}$ (Gutmark & Wygnanski 1976) as also required above. The plane jet can therefore be concluded to be self-similar in terms of $U_m$ and $y_{1/2}$.

## 3.4. Simulation results

In all wall-jet simulations the inlet Reynolds and Mach numbers are $Re = U_j h/\nu_j = 2000$ and $M = U_j/a_j = 0.5$, where $h$ is the inlet jet height and the index $j$ is used to denote properties at the inlet jet center. Above the jet a constant coflow of $U_c = 0.10U_j$ is applied and at the top of the domain a slight inflow condition is used to account for the entrainment of ambient fluid during turbulent propagation. To achieve a plane wall-jet periodic boundary conditions are applied in the spanwise $z$-direction.

### 3.4.1. *Isothermal wall-jet including scalar mixing*

In Ahlman *et al.* (2007*a*) the development of a plane turbulent wall-jet is studied using DNS. The jet is isothermal and inlet disturbances are added to facilitate efficient transition to turbulence. In order to study mixing, a passive scalar added in the jet is solved for. A zero flux condition at the wall is applied for the scalar. As the jet propagates downstream the jet undergoes transition to turbulence and approximately downstream of $x/h = 11$ the jet is fully turbulent. The development of the simulated half-width is linear and approximately $dy_{1/2}/dx = 0.068$. Separate inner and outer scalings were applied to investigate the self-similarities of the respective layers. In the near-wall layer conventional wall variables are able to collapse statistics profiles and this region therefore resembles that of a zero pressure-gradient boundary layer. Mean streamwise velocity profiles in inner scaling are shown in figure 3.3 where the profiles in the viscous sublayer $y^+ < 5$ are seen to collapse. The Reynolds number of the simulation is however too low for a logarithmic region to develop. In the outer layer, $y > y_m$, the averaged statistics collapse when scaled by the half-width and the outer excess velocity $(U_m - U_c)$, as is seen in figure 3.4. This implies that the outer layer development is similar to that of a plane jet. Regarding the mixing, the scalar half-width also develops linearly. The scalar fluctuation intensity in the outer layer corresponds to values found in plane jets, and the streamwise and wall-normal scalar fluxes are of comparable magnitude. This implies that the scalar flux vector is not aligned with the mean scalar gradient, which to a close approximation is normal to the wall. The profiles of the mechanical to mixing time scale at different downstream positions also collapse in the outer layer.

Early results from the simulation of the isothermal wall-jet including scalar mixing were presented at the Fourth International Symposium on Turbulence and Shear Flow Phenomena in Williamsburg, Virginia, USA in 2005 (Ahlman *et al.* 2005). Results from the final simulation were presented in part at the $6^{th}$ Euromech Fluid Mechanics Conference in Stockholm, Sweden, (Ahlman *et al.* 2006) and the full results including their discussion are published in the enclosed Paper 1 (Ahlman *et al.* 2007*a*).

### 3.4.2. *Non-isothermal wall-jets*

In Ahlman *et al.* (2007*b*) two non-isothermal wall-jets are studied. A warm jet in a cold surrounding and a cold jet in a warm surrounding are simulated, and the results are compared to those obtained in the isothermal case described above. Significant density differences are used to mimic the situation in cooling or combustion situations. The warm jet case resembles a situation of warm exhaust gas flowing over a cold wall while the cold jet can be seen as an idealized thin film cooling situation.

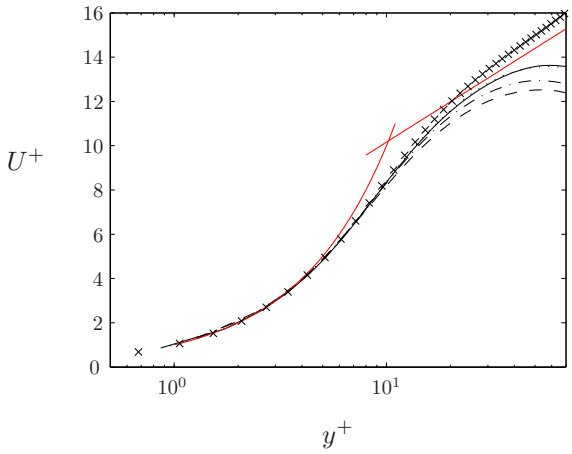


FIGURE 3.3. Mean streamwise velocity profiles in inner scaling ($U^+ = U/u_\tau$, $y^+ = yu_\tau/\nu$) at different downstream positions; $x/h = 15$ (dashed), $x/h = 20$ (dashed-dotted), $x/h = 30$ (dotted) and $x/h = 40$ (solid). The viscous relation $U^+ = y^+$, the logarithmic inertial relation $U^+ = \frac{1}{0.38}\ln(y^+) + 4.1$ from Österlund (1999) and DNS data at $Re_{\delta^*} = 200$ by Skote *et al.* (2002) ($\times$) are also shown.

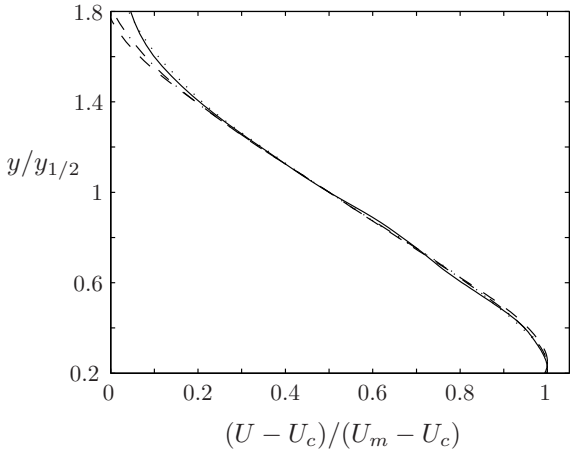


FIGURE 3.4. Mean streamwise velocity profiles in the outer shear layer, using outer scaling adjusted for the coflow. Lines as in fig. 3.3.

For a direct comparison the same setup as in the isothermal study is used, including equal inlet Reynolds and Mach numbers and the same inlet disturbances. As in the isothermal simulation above a passive scalar is added at the

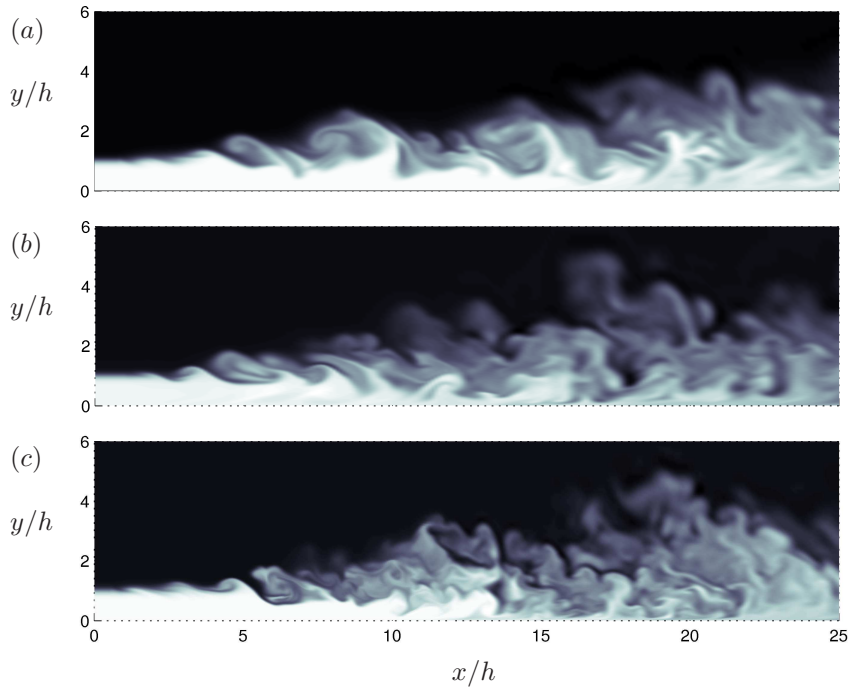


FIGURE 3.5. Snapshots of the passive scalar concentration $\theta/\Theta_j$ in the cold ($a$), isothermal ($b$) and warm jet ($c$) in the simulations of Ahlman *et al.* (2007*b*).

inlet, enabling an investigation of both a passive and an active scalar (heat) mixing. The temperature and density in the coflow and at the wall are equal and constant. The non-isothermal jets are characterized by the ratio of the ambient and jet density at the inlet $\alpha_\rho = \rho_a/\rho_j$. In the warm jet $\alpha_\rho = 1.7$ corresponding to a temperature difference of $205.1K$ while in the cold jet $\alpha_\rho = 0.4$ with a corresponding temperature difference of $439.5K$. The fluid viscosity varies with temperature according to Sutherland's law (Sutherland 1893).

The most striking influence of the varying density is on the turbulence structures and the range of scales in the jets. This effect can be seen in figure 3.5 showing snapshots of the passive scalar concentration in the cold, isothermal and warm jet. The warm jet contains the largest range of scales and has significantly more small scale energy than the other two cases. Correspondingly, the cold jet contains the smallest range of scales and the least amount of small scale energy. This is a result of the varying density and can be understood by observing the friction Reynolds number $Re_\tau = \delta/l^* = \delta/(\nu_w/u_\tau)$, which provides an estimate of the outer to inner length scale ratio. For the wall-jets $\delta = y_{1/2}$ is

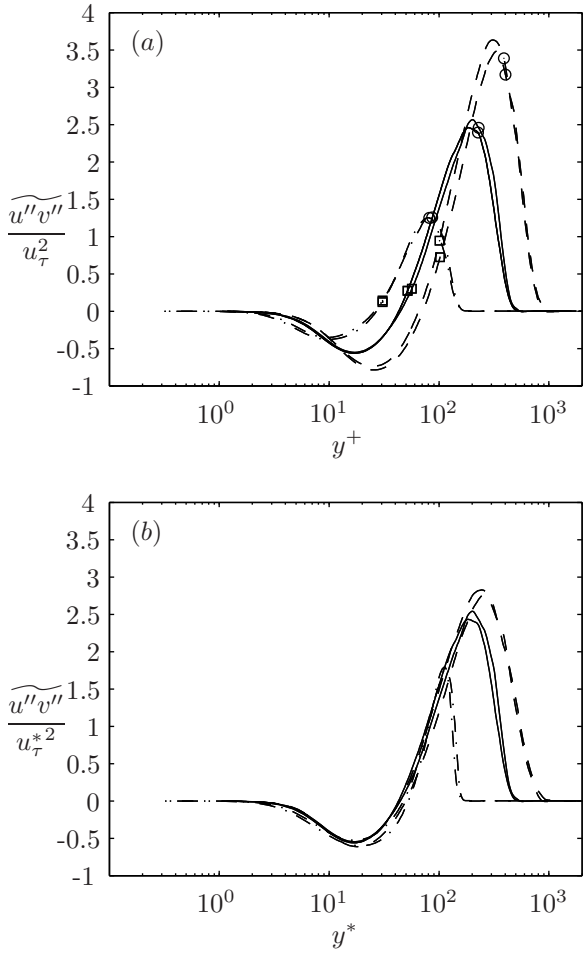


FIGURE 3.6. Reynolds shear stress, using boundary layer scaling ($a$) and semi-local scaling ($b$) in the isotherm (solid), warm (dashed), and cold jet (dash-dotted) in Ahlman *et al.* (2007*b*). Profiles at $x/h = 20$ and $x/h = 25$. In ($a$) symbols mark the $U_m$ ($\square$) and $y_{1/2}$ ($\circ$) positions.

an appropriate choice. In the warm jet the viscosity decreases towards the relatively colder wall, decreasing the viscous length scale and increasing the scale separation. The opposite occurs in the cold jet. In the fully turbulent region $Re_\tau$ is about 4.5 times higher in the warm jet than in the cold. Another result of the varying density is that the conventional wall scaling fails to collapse inner layer statistics from the three cases. An improved collapse can be reached by applying 'semi-local' scaling (Huang *et al.* 1995) where the wall variables

are based on the local density and viscosity. In figure 3.6 the Reynolds shear stress in the three cases are seen in conventional wall variables and in semi-local scaling. In this case the semi-local scaling collapses the data over the entire inner layer. The profiles of the mean and fluctuating velocities are significantly different in the non-isothermal cases but the differences between Reynolds and Favre (density-weighted) averages are small. This indicates that the compressibility effects mainly are a result of the varying mean density. Concerning the mixing, the turbulent Schmidt and Prandtl number vary significantly only in the near-wall layer and in a small region below the jet center. In the outer part they are approximately constant. The scalar dissipation rate of both the passive scalar and the temperature is studied. In the inner layer the dissipation rates are different due to the different boundary conditions. In the outer layer the cold jet dissipation rate has a different behavior due to the very low Reynolds number. The ratio of the mechanical to passive scalar time scale is approximately equal in the outer layer.

Results from the non-isothermal simulations were presented in part at the Fifth International Symposium on Turbulence and Shear Flow Phenomena in Munich, Germany (Ahlman *et al.* 2007*c*). The results and their interpretation are presented in full in the enclosed Paper 2 (Ahlman *et al.* 2007*b*).

### 3.4.3. *Reacting wall-jet*

In the final study a reacting turbulent wall-jet is simulated. The same flow setup as in the previous studies is used, including the flow field inlet conditions and disturbances. The simulated reaction is a single irreversible reaction between an oxidizer and a fuel forming a product, as described by $O + F \longrightarrow P$. The jet is isothermal and no heat is released during the reaction. At the inlet the fuel and oxidizer are separated. Fuel is injected in the jet while the oxidizer is added in the coflow. The reaction rate is constant, independent of temperature and is prescribed by a Damköhler number of $Da = hk_r\rho_j/U_j = 3$. The convection and reaction time scale are hence of the same order. A non-reacting scalar equation is also solved to facilitate comparison of reacting and non-reacting statistics.

For the reacting simulation comparison of the flow development and the passive scalar statistics show that the results in general compare well with the previous non-reacting simulation (Ahlman *et al.* 2007*a*). The reaction in the simulation occurs mainly in the upper shear layer in thin sheet like structures highly convoluted by the high intensity fluctuations. A snapshot of the reaction can be seen in figure 3.7. Due to the turbulent mixing the reaction occurs also in the inner shear layer, but to a lesser extent, which can also be seen in the snapshot. The maximum reaction rate occurs at the half-width $y_{1/2}$ as is seen in figure 3.8a. In figure 3.8b the reacting and non-reacting scalars are shown. The reacting scalar concentration decrease due to the reaction, especially in the outer layer. The mean gradients of the reactants are consequently increased.

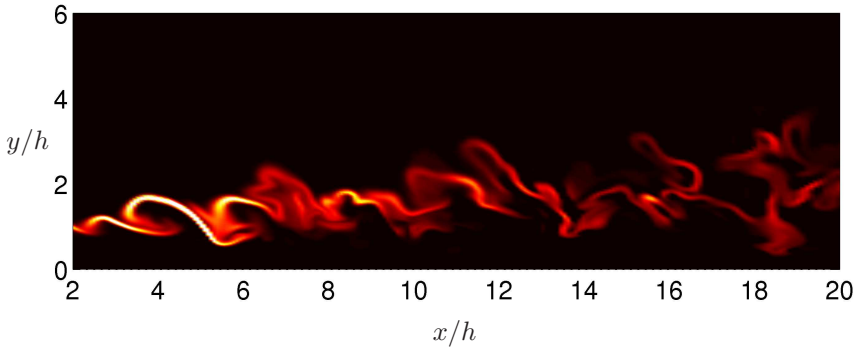


FIGURE 3.7. Inlet normalized reaction rate $\dot{\omega}$. Light color represent high reaction rate.

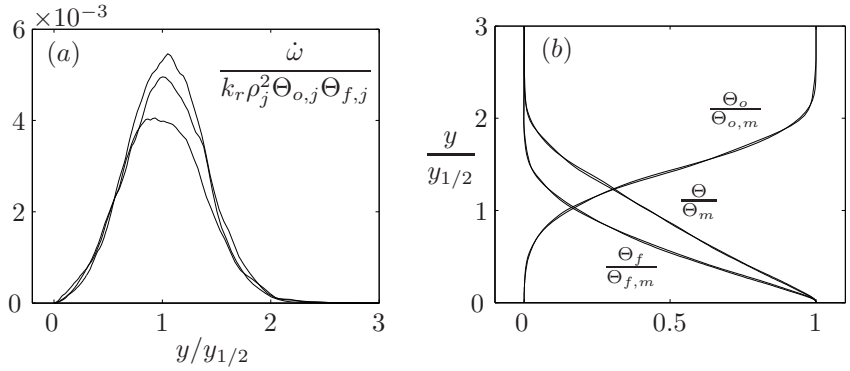


FIGURE 3.8. Mass reaction rate at $x/h = 15, 17, 20$ $(a)$ and mean scalar profiles at $x/h = 17$ & $20$ $(b)$.

# Outlook

The code developed is capable of simulating mixing and reaction in a plane wall-jet, as have been shown in the performed investigations. It can also handle significant density differences. A logical next step is to carry out DNS of combustion, using temperature dependent reaction rates and realistic heat release. Because of computational limitations only simple reaction mechanisms seem to be realistic. The need for a fully compressible solution may also be considered. If small compressible effects can be anticipated, a low Mach number formulation could possibly be used instead to relax the need for small time steps. By simulating a turbulent wall-jet along a cold wall, the effects of a heat flux on the reactions could be investigated. It is of interest to study when or how local quenching occurs. How far away from the wall can it occur and how is it affected by the reaction rate and the degree of premixing? In short, how is the mixing and reaction dynamics influenced by a cold wall? Statistics generated for this case could also be used to evaluate and develop combustion model approaches.

# Acknowledgements

The present work has been a part of and funded by the national Research Program within The Centre for Combustion Science and Technology (CECOST). Funding for CECOST has been provided by the Swedish Energy Agency (Energimyndigheten). The funding is greatfully acknowledged! The computing time used was granted by the Swedish National Infrastructure for Computing (SNIC) through the Swedish National Allocation Committee (SNAC), and the simulations were carried out using resources at The Center for Parallel Computers (PDC) at The Royal Institute of Technology (KTH). All parties are thanked for their time and effort!

I would like to express my deepest gratitude to my supervisors for their constant support. Thank you Arne for always having a positive mind set, and for constantly sharing your insights in scientific research in general and your knowledge in turbulence in particular. Thank you Geert for taking the time to discuss any and all issues of fluid mechanics. Also for almost instantly providing feedback on my work and thereby improving it significantly.

I would like to thank Henrik Alfredsson, Espen Åkervik, Gunnar Tibert and Tony Burden for providing valuable feedback on the thesis. Bendiks Jan Boersma is thanked for providing the original version of the simulation code. All friends and colleagues at the Mechanics department are thanked for creating a friendly and inspiring atmosphere.

*Jag vill tacka alla vänner (ni vet vilka ni är) och min familj för all kärlek och omtänksamhet! Hej mormor!*

*Sofia, du är fantastisk!*

# Bibliography


Ahlman, D., Brethouwer, G. & Johansson, A. V. 2005 Direct numerical simulation in a plane compressible and turbulent wall jet. In *Fourth international symposium on Turbulence and Shear Flow Phenomena*, pp. 1131–1136.

Ahlman, D., Brethouwer, G. & Johansson, A. V. 2006 Simulation and evaluation of mixing in a plane compressible wall-jet. In *Euromech Fluid Mechanics Conference 6*, p. 109.

Ahlman, D., Brethouwer, G. & Johansson, A. V. 2007*a* Direct numerical simulation of a plane turbulent wall-jet including scalar mixing. *Phys. Fluids* **19**, 065102.

Ahlman, D., Brethouwer, G. & Johansson, A. V. 2007*b* Direct numerical simulation of non-isothermal turbulent wall-jets. *Phys. Fluids* (Submitted).

Ahlman, D., Brethouwer, G. & Johansson, A. V. 2007*c* Direct numerical simulation of non-isothermal turbulent wall-jets. In *Fifth international symposium on Turbulence and Shear Flow Phenomena*, pp. 1293–1299.

Ahlman, D., Brethouwer, G. & Johansson, A. V. 2007*d* A numerical method for simulation of turbulence and mixing in a compressible wall-jet, version 2. *Tech. Rep*. Linné Flow Centre, Dept. of Mechanics, Royal Institute of Technology.

Arrhenius, S. 1889 Über die Reaktionsgeschwindigkeit bei der Inversion von Rohrzucker durch Saüren. *Z. Physik. Chem.* **4**, 226–248.

Bilger, R. W. 2000 Future progress in turbulent combustion research. *Prog. Energy Combust. Sci.* **26**, 367–380.

Boersma, B. J. 2004 Numerical simulation of the noise generated by a low Mach number, low Reynolds number jet. *Fluid Dyn. Res.* **35**, 425–447.

Bradshaw, P. & Gee, M. T. 1960 Turbulent wall-jets with and without external stream. *Aero. Res. Council R&M 3252* .

Bruneaux, G., Akselvoll, K., Poinsot, T. & Ferziger, J. H. 1996 Flame-wall interaction simulation in a turbulent channel flow. *Combust. Flame* **107**, 27–44.

Bruneaux, G., Poinsot, T. & Ferziger, J. H. 1997 Premixed flame-wall interaction in a turbulent channel flow: budget for the flame surface density evolution equation and modeling. *J. Fluid Mech.* **349**, 191–219.

Conaire, M. O., Curran, H. J., Simmie, J. M., Pitz, W. J. & Westbrook, C. K. 2004 A comprehensive modeling study of hydrogen oxidation. *Int. J. Chem. Kinet.* **36**, 603–622.

Curran, H. J., Gaffuri, P., Pitz, W. J. & Westbrook, C. 2002 A comprehensive modeling study of iso-octane oxidation. *Combust. Flame* **129**, 253–280.

Dabrieau, F., Cuenot, B., Vermorel, O. & Poinsot, T. 2003 Interaction of flames of $H_2 + O_2$ with inert walls. *Combust. Flame* **135**, 123–133.

Dejoan, A. & Leschziner, M. A. 2005 Large eddy simulation of a plane turbulent wall jet. *Phys. Fluids* **17**, 025102.

Ehn, A., Kaldvee, B., Bood, J. & Aldén, M. 2007 *Private Communication* Div. of Combustion Physics, Lund University, Sweden.

Eriksson, J. G., Karlsson, R. I. & Persson, J. 1998 An experimental study of a two-dimensional plane turbulent wall jet. *Exp. Fluids* **25**, 50–60.

Förthmann, E. 1936 Turbulent jet expansion. *NACA TM* **789**, (English Translation).

George, W. K., Abrahamsson, H., Eriksson, J., Karlsson, R. I., Löfdahl, L. & Wosnik, M. 2000 A similarity theory for the turbulent plane wall jet without external stream. *J. Fluid Mech.* **425**, 367–411.

Glassman, I. 1996 *Combustion*, 3rd edn. Academic Press.

Guldberg, C. M. & Waage, P. 1864 Studies concerning affinity. *C. M. Forhandlinger: Videnskabs-Selskabet i Christiana* **35**.

Gutmark, E. & Wygnanski, I. 1976 The planar turbulent jet. *J. Fluid Mech.* **73**, 465–495.

Hilbert, R., Tap, F., El-Rabii, H. & Thévnin, D. 2004 Impact of detailed chemistry and transport models on turbulent combustion. *Prog. Energy Combust. Sci.* **30**, 61–117.

Huang, P. G., Coleman, G. N. & Bradshaw, P. 1995 Compressible turbulent channel flows: DNS results and modelling. *J. Fluid Mech.* **305**, 185–218.

Klein, M., Sadiki, A. & Janicka, J. 2003 A digital filter based generation of inflow data for spatially developing direct numerical or large eddy simulations. *J. Comp. Phys.* **186**, 652–665.

Klimenko, A. Y. & Bilger, R. W. 1999 Conditional moment closure for turbulent combustion. *Prog. Energy Combust. Sci.* **25**, 595–687.

Kou, K. K. 2005 *Principles of Combustion*, 2nd edn. John Wiley.

Launder, B. E. & Rodi, W. 1981 The turbulent wall jet. *Prog. Aerospace Sci.* **19**, 81–128.

Launder, B. E. & Rodi, W. 1983 The turbulent wall jet – measurements and modelling. *Annu. Rev. Fluid Mech.* **15**, 429–459.

Levin, O., Chernoray, V. G., Löfdahl, L. & Henningson, D. 2005 A study of the blasius wall jet. *J. Fluid Mech.* **539**, 313–347.

Levin, O., Herbst, A. & Henningson, D. 2006 Early turbulent evolution of the blasius wall jet. *J. Turb.* **7**, 1–17.

McMurtry, P. A., Riley, J. J. & Metcalfe, R. W. 1989 Effects of heat release on the large-scale structure in turbulent mixing layers. *J. Fluid Mech.* **199**, 297–332.

Miller, M. S., Madina, C. K. & Givi, P. 1994 Structure of a turbulent reacting mixing layer. *Comb. Sci. Tech.* **99**, 1–33.

Mizobuchi, Y., Shinjo, J., Ogawa, S. & Takeno, T. 2005 A numerical study on the formation of diffusion flame islands in a turbulent hydrogen jet lifted flame. *Proc. Combust. Inst.* **30**, 611–619.

Muñiz, L. & Mungal, M. G. 2001 Effects of heat release and buoyancy on flow structure and entrainment in turbulent nonpremixed flames. *Comb. and Flame* **126**, 1402–1420.

Narashima, R., Narayan, K. Y. & Parthasarathy, S. P. 1973 Parametric analysis of turbulent wall jets in still air. *Aeronaut. J.* **77**, 335–359.

Österlund, J. M. 1999 Experimental studies of zero pressure-gradient turbulent boundary layer flow. PhD thesis, Royal Institute of Technology, KTH.

Pantano, C. 2004 Direct simulation of non-premixed flame extinction in a methane-air jet with reduced chemistry. *J. Fluid Mech.* **514**, 231–270.

Pantano, C., Sarkar, S. & Williams, F. A. 2003 Mixing of a conserved scalar in a turbulent reacting shear layer. *J. Fluid Mech.* **481**, 291–328.

Peters, N. 1985 *Numerical and asymptotic analysis of systematically reduced reaction schemes for hydrocarbon flames*, *Lecture notes in physics*, vol. 241, pp. 90–109. Springer.

Peters, N. 1986 Laminar flamelet concepts in turbulent combustion. In *Twenty-First Symposium (Int.) on Combustion*, pp. 1231–1250. The Combustion Institute, Pittsburgh.

Peters, N. 2000 *Turbulent Combustion*. Cambridge University Press.

Pitsch, H. 2006 Large-eddy simulation of turbulent combustion. *Annu. Rev. Fluid Mech.* **38**, 453–482.

Poinsot, T., Candel, S. & Trouvé, A. 1996 Applications of direct numerical simulation to premixed turbulent flames. *Prog. Energy Combust. Sci.* **21**, 531–576.

Poinsot, T., Haworth, D. C. & Bruneaux, G. 1993 Direct simulation and modeling of flame-wall interaction for premixed turbulent combustion. *Combust. Flame* **95**, 118–132.

Poinsot, T. & Veynante, D. 2001 *Theoretical and Numerical Combustion*. R.T. Edwards.

Pope, S. B. 1985 PDF methods for turbulent reactive flows. *Prog. Energy Combust. Sci.* **11**, 119–192.

Pope, S. B. 2000 *Turbulent Flows*. Cambridge University Press.

Riley, J. J., Metcalfe, R. W. & Orszag, S. A. 1986 Direct numerical simulation of chemically reacting turbulent mixing layers. *Phys. Fluids* **29**, 406–422.

Seyfried, H., Särner, G., Omrane, A., Richter, M., Schmidt, H. & Aldén, M. 2005 Optical diagnostics for characterization of a full-size figther-jet afterburner. In *ASME Turbo Expo*. GT2005-69058.

Skote, M., Haritonidis, J. H. & Henningson, D. 2002 Varicose instabilities in turbulent boundary layers. *Phys. Fluids* **14**, 2309–2323.

Spalding, D. 1971 Mixing and chemical reaction in steady confined turbulent flames. In *Thirteenth Symposium (Int.) on Combustion*, pp. 649–657. The Combustion Institute, Pittsburgh.

Sutherland, W. 1893 The viscosity of gases and molecular force. *Phil. Mag.* **36**, 507–531.

Tanahashi, M., Fuhimura, M. & Miyauchi, T. 2000 Coherent fine-scale eddies in turbulent premixed flames. *Proc. Comb. Inst.* **28**, 529–535.

Tennekes, H. & Lumley, J. L. 1972 *A first course in turbulence*. The MIT Press.

Treurniet, T. C., Nieuwstadt, F. T. M. & Boersma, B. J. 2006 Direct numerical simulation of homogeneous turbulence in combination with premixed combustion at low mach number modelled by the G-equation. *J. Fluid Mech.* **565**, 25–62.

Verbiezen, K., Donkerbroek, A. J., Klein-Douwel, R. J. H., van Vliet, A. P., Frijters, P. J. M., Seykens, X. L. J., Baert, R. S. G., Meerts, W. L., Dam, N. J. & ter Meulen, J. J. 2007 Diesel combustion: In-cylinder NO concentrations in relation to injection timing. *Comb. and Flame* **151**, 333–346.

Vervisch, L. & Poinsot, T. 1998 Direct numerical simulation of non-premixed turbulent flames. *Annu. Rev. Fluid Mech.* **30**, 655–691.

Veynante, D. & Vervisch, L. 2002 Turbulent combustion modeling. *Prog. Energy Combust. Sci.* **28**, 193–266.

Visbal, M., Gaitonde, D. V. & Gogineni, S. P. 1998 Direct numerical simulation of a forced transitional plane wall jet. *AIAA Paper* 98-2643.

Wang, Y. & Trouvé, A. 2005 Direct numerical simulation of nonpremixed flame-wall interactions. *Combust. Flame* **144**, 461–475.

Westbrook, C. K., Mizobuchi, Y., Poinsot, T. J., Smith, P. J. & Warnatz, J. 2005 Computational combustion. *Proc. Combust. Inst.* **30**, 125–157.

Wikström, P. M., Wallin, S. & Johansson, A. V. 2000 Derivation and investigation of a new explicit algebraic model for the passive scalar flux. *Phys. Fluids* **12**, 688–702.

Williams, F. A. 1985 *Combustion Theory*, 2nd edn. Benjamin/Cummings.